

Once more on the interrelation between Abelian monopoles and P-vortices in $SU(2)$ LGT

P. Yu. Boyko[†], V. G. Bornyakov^{†,*}, E.-M. Ilgenfritz^{**}, A. V. Kovalenko[†],
B. V. Martemyanov[†], M. Müller-Preussker^{**}, M. I. Polikarpov[†] and
A. I. Veselov[†]

[†] *Institute of Theoretical and Experimental Physics,
B. Chermushkinskaya 25, Moscow, 117259, Russia*

^{*} *Institute for High Energy Physics,
Protvino, 142281, Russia*

^{**} *Institut für Physik, Humboldt-Universität,
Newtonstrasse 15, 12489 Berlin, Germany*

Abstract

We study the properties of configurations from which P-vortices on one hand or Abelian monopoles on the other hand have been removed. We confirm the loss of confinement in both cases and investigate in what respect the modified ensembles differ from the confining ones from the point of view of the complementary confinement scenario.

1 Introduction

There are two popular phenomenological explanations of confinement in lattice gluodynamics: the monopole [1] and the center vortex [2, 3, 4, 5, 6, 7, 8] confinement mechanism that have been critically discussed in Ref. [9]. Monopoles and center vortices are defined by projection to $U(1)^{N-1}$ or $Z(N)$ gauge fields, respectively. Hence, the center vortices are called P-vortices in order to emphasize the difference from extended (continuum) vortices¹. These two types of excitations reproduce, respectively, about 90% [10] and about 70% [11] of the non-Abelian string tension and are able to explain other nonperturbative properties. Therefore, removing monopole fields [12, 13] or P-vortices [14] should leave only inert gauge field configurations, unable to confine external charges or to break chiral symmetry.

It was very attractive to conjecture [15, 16] that monopoles and P-vortices are geometrically interrelated. Indeed, this was found to be the case in $SU(2)$ gluodynamics: more than 90% of monopole currents are localized on the P-vortices [16, 17, 18]. One of our goals in the present paper is to elaborate on this interrelation between monopoles and vortices.

In Ref. [14] the operation of center vortex (P-vortex) removal has been invented, and it was demonstrated that the quark condensate and the topological charge are destroyed thereby. Later it has been found [19] that the number of links that have to be modified in this operation can be essentially reduced when the $Z(2)$ gauge freedom is used to minimize the number of negative trace links. The remaining negative links can be interpreted in terms of three-dimensional domains.

The operation of monopole removal has been invented by Miyamura et al. in Ref. [12, 13]. It has been shown that not only the quark condensate and the topology is destroyed thereby, but that the Abelian monopole field alone, completed again by the non-diagonal gluons, carries all necessary degrees of freedom in order to allow the reconstruction of chiral symmetry breaking and topological charge.

All technical details (including those of gauge fixing) relevant for our study are relegated to the Appendix.

Ph. de Forcrand and M. D'Elia [14] were the first to ask what happens to the Abelian monopoles when P-vortices are removed. We have started our work from the opposite question: what remains from the center vortex degrees of freedom when Abelian monopoles are subtracted from the Abelian part of the gauge fields. Originally, it was only for completeness that we also repeated the study of Ref. [14]. Not unexpectedly, we found that the results depend on the method of gauge fixing and details of its algorithmic implementation. But turning again to de Forcrand's and D'Elia's problem with the perfectionated gauge fixing has resulted in a paradox that has led us to a closer investigation what properties the network of monopole world lines must possess in order to confine.

Most of the above mentioned results in the literature was obtained for the Direct Center Gauge (DCG) [4] and for the Indirect Center Gauge (ICG) [2]. In the present paper we also use both of them. The Laplacian center gauge [20], also used for studies of the P-vortices, is not studied here. Although the absence of the Gribov ambiguity is a virtue of this gauge, we consider the absence of scaling of the resulting density of P-vortices [21] as a less appealing feature. We have been doing all gauge fixings by means of simulated annealing, repeating however the procedure for a number of copies. In this respect we have done our best (according to the present state of the art) to circumvent the infamous Gribov ambiguity.

¹We will interchangeably use both terms in the following.

In all studies described in this paper we have used a confining ensemble of 100 configurations on a $24^3 \times 6$ lattice, generated at $\beta = 2.35$ using the Wilson action. This corresponds to a lattice spacing given by $a \sqrt{\sigma} = 0.3108(17)$ [22]², in other words, to a temperature $T/T_c = 0.7562(80)$, where the ratio $T_c/\sqrt{\sigma} = 0.7091(36)$ (obtained for $SU(2)$ gluodynamics with Wilson action in Ref. [23]) has been used. Adopting the standard value of the string tension, $\sigma = (440\text{MeV})^2$, the estimated lattice spacing would be $a = 0.139(1)$ fm, resulting in a spatial volume of $(3.336 \text{ fm})^3$.

In order to demonstrate the confining property or the loss of confinement in the case of finite temperature adopted here, we use the correlator of the Polyakov loop,

$$aV(r) = -\frac{1}{N_\tau} \log \langle P(\vec{x}) P^*(\vec{y}) \rangle \quad (1)$$

with $r = |\vec{x} - \vec{y}|$. Strictly speaking, this is the excess free energy related to the presence of a quark-antiquark pair. For simplicity we will call it potential, however. For the full non-Abelian potential the Polyakov loop

$$P(\vec{x}) = \frac{1}{2} \text{Tr} \prod_{t=1}^{N_\tau} U_{\vec{x},t,4} \quad (2)$$

is used. When the monopole-generated potential shall be sorted out, the monopole part of the Abelian Polyakov loop,

$$P^{mon}(\vec{x}) = \text{Re exp} \left(\sum_{t=1}^{N_\tau} i\theta_{\vec{x},t,4}^{mon} \right) = \cos \left(\sum_{t=1}^{N_\tau} \theta_{\vec{x},t,4}^{mon} \right), \quad (3)$$

is entering the correlator. The monopole part of the gauge field $\theta_{x,\mu}^{mon}$ is defined in eq. (13) in the Appendix. Finally, in order to measure the vortex contribution to the potential, the Polyakov loop is constructed in terms of the $Z(2)$ projected links

$$P^{vort}(\vec{x}) = \prod_{t=1}^{N_\tau} Z_{\vec{x},t,4}, \quad (4)$$

with $Z_{x,\mu}$ defined in eq. (8) in the Appendix.

As already said, in the course of the present paper, we are studying monopole currents in configurations where the P-vortices are removed and P-vortices in configurations where the monopoles are removed. The results are trivial for the case of ICG, as we will show in Section 3. Here, only nonpercolating monopole currents or only small, nonpercolating center vortices, respectively, are left over.

Note that in the Laplacian center gauge the monopoles are located on the center vortices [20] and thus removal of the vortices automatically leads to removal of the monopoles. We expect that, similar to ICG, removal of monopoles in this gauge will give rise to nonpercolating center vortices.

In the case of DCG, when the emerging center vortices are removed, the situation is more challenging (as described in Section 4). We observed that removing P-vortices leads to gauge field configurations with monopole currents even more dense and still percolating although confinement is lost. This is possible since monopole and vortex degrees of freedom are, at first sight, only loosely connected in DCG, in contrast to ICG. This intriguing observation has prompted us to search for the necessary conditions for monopole percolation to generate confinement. We found

²We thank Mike Teper for confirming that this value actually refers to $\beta = 2.35$.

the reason why monopole percolation, although necessary, is not sufficient to create a non-vanishing string tension. We shall argue below that this effect is due to a very special structure of the percolating monopole cluster: it is highly correlated at small distances which screens monopole currents more than this is the case in normal configurations.

Finally, in Section 5, we analyse how the subtraction of singular components in the Abelian gauge field (generated by monopoles) changes the P-vortex structure. In Section 6 we draw some conclusions.

2 Monopole and vortex percolation

The paradox mentioned in the Introduction is the observation that monopole percolation is not sufficient to guarantee confinement. This is surprising because monopole percolation has become synonymous for monopole condensation. The monopole condensation mechanism of confinement has been, together with the Dual Superconductor picture, proposed by 't Hooft [24] and Mandelstam [25] implying that long-range physics is dominated by Abelian degrees of freedom (Abelian dominance). Gauge fixing and Abelian projection have been suggested [26] as a method to verify this idea. On the lattice this has been first implemented in Ref. [27].

When Abelian dominance of the string tension had been verified on the lattice [28], this has boosted the development in two directions. At first, several observables have been constructed in terms of the monopole currents (which are immediately available in the projected theory) serving the intention that each of them should reflect the phenomenon of monopole condensation. In this paper we will not comment on the second direction, the construction of a true monopole condensation disorder parameter, following the early proposals in Refs. [29, 30]. This observable should have a non-vanishing expectation value in the confining phase (hopefully independently of the particular Abelian projection [26]) indicating the spontaneous breakdown of the corresponding magnetic $U(1)$ symmetry of the latter [31, 32, 33].

Returning to the direct monopole observables in MAG, the first proposal was to measure the monopole current density ρ_{mon} and to establish its scaling property with respect to β at zero temperature [34]. The monopole density and similarly the vortex density are defined as

$$\rho_{\text{mon}} = \frac{\langle N_{\text{mon}} \rangle}{4N_s^3 N_\tau} \quad \text{and} \quad \rho_{\text{vort}} = \frac{\langle N_{\text{vort}} \rangle}{6N_s^3 N_\tau}, \quad (5)$$

where N_{mon} is the number of dual links occupied by monopole currents and N_{vort} the number of dual plaquettes belonging to the vortex area.

The observed scaling of the monopole density has later found to be premature. Moreover, the density lacks scaling and universality [35, 36] and requires to be separated into “ultraviolet” and “infrared component”, the scaling behavior of which is different, meaning that the UV component reflects only short distance artefacts without relevance for confinement. Only the IR component turned out to be scaling and relevant for condensation [37] and for confinement. Relatively soon after the first quantitative study of ρ_{mon} [34], the focus has turned to structural properties of the network of monopole currents, which has found to be clearly undergoing a change at the deconfinement phase transition [38]. The change concerned the distribution of connected clusters with respect to the length L (*i.e.* the number of participating monopole currents). This distribution is denoted as $N(L)$ and counts

the number of connected clusters of given size L in the ensemble of configurations. In [38], and later in Refs. [39] and [40, 41] it has been clearly demonstrated that, in the confinement phase, each configuration contains a single macroscopic cluster (in modern parlance the “infrared monopole component”) of many connected dual links carrying non-vanishing monopole current, apart from a big number of small clusters (the “ultraviolet monopole component”). The macroscopic clusters were found to be *percolating*. This is meant in the sense that they are impossible to enclose in a 4D cuboid smaller than the periodic lattice in one or more directions or in the sense of a cluster two-point function [37] not to vanish at “infinite” distance. Obviously, this notion of percolation does not take into recognition the orientation of the monopole currents. The eventual occurrence of more than one macroscopic cluster was found to be an effect of smaller volume.

Of course, it is not difficult just to evaluate Wilson loops under the influence of the Abelian field due to all monopole currents [1, 42, 43], a procedure that clearly takes the orientation into account. In this way, monopole dominance [1, 10] has been demonstrated. Later it has been found that the macroscopic clusters (and only these) build up the Abelian string tension [41]. The essence of the deconfinement transition in this light had already earlier been identified [38] as the decomposition of the macroscopic cluster into many smaller ones, *i.e.* a qualitative change of the size distribution of the clusters, accompanied by the generation of an anisotropy of the current density. In the Euclidean time direction, the percolation property of the remaining larger clusters persists above T_c , whereas there is no percolation anymore in the spatial directions.

All this contributed to the common belief that spacelike percolation is a necessary *and* sufficient condition for confinement. In this paper we find an interesting counter example showing that a percolating cluster does not necessarily confine, as the direct evaluation of the monopole contribution to the Wilson loops reveals.

In the case of the P-vortex mechanism, the direct evaluation of their contribution to Wilson loops (by a factor $(-1)^{\text{linking number}}$ for each vortex), the fact of center dominance (of the string tension) and the scaling property of the P-vortex density ρ_{vort} (being equal to the density of negative plaquettes) have been emphasized from the very beginning [5]. Also here, the existence of one macroscopic P-vortex, a closed surface consisting of many dual plaquettes, was found to be a prerequisite of confinement, and this P-vortex itself was found percolating [44] in all directions. The deconfinement transition was later identified, in analogy to the monopole mechanism, with a de-percolation transition [45, 7, 46], *i.e.* with the macroscopic vortex being replaced by smaller ones. If big enough, these are percolating in the time direction, but no more in spatial directions.

In our investigation, for P-vortices we did not find any indication that vortices would persist to be spatially percolating in the case confinement has been destroyed (*e.g.* by the removal of monopoles).

3 Indirect center gauge

ICG fixing includes two steps. First, the maximally Abelian gauge (MAG) is fixed and Abelian projection is made. Then the Abelian gauge fields (and the remaining Abelian gauge invariance) are used to fix the (Abelian) maximal center gauge. After the center projection is made, the emerging $Z(2)$ configuration is looked up for negative links $Z_{x,\mu} = -1$ (see Appendix for further details). In Fig. 1 the length spectrum $N(L)$ of the monopole clusters, obtained after fixing the MAG, is

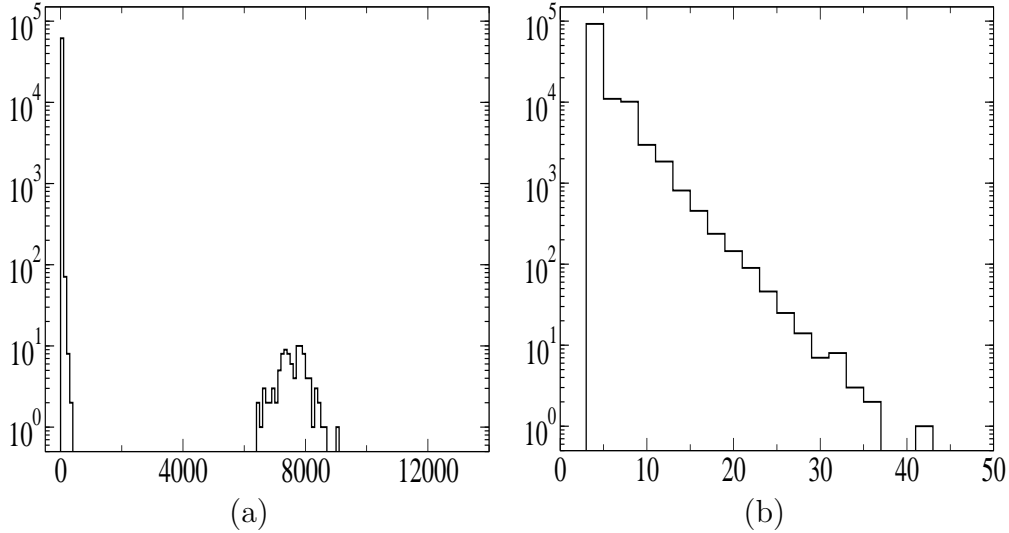


Figure 1: The monopole clusters length distribution $N(L)$ for Wilson $\beta = 2.35$ on 24^{36} lattices before (a) and after (b) removing the center vortices found according to ICG.

compared with the same spectrum after the P-vortices have been removed. More precisely, here and later $N(L)$ represents the number of clusters of size L found in all 100 configurations. Note, that the vortex removal operation consists in changing the sign of links with negative $\cos(\theta_{x,\mu})$ in the (Abelian) maximal center gauge, and that this operation preserves the MAG [10].

The original monopole density (per dual link) is $\rho_{\text{mon}} = 0.0357 \pm 0.0002$ and the original vortex (area) density (per dual plaquette) is $\rho_{\text{vort}} = 0.0805 \pm 0.0002$.

It is seen that the percolating monopole clusters with length around 7,000 that are present before in each lattice configuration, are absent from the length spectrum after the vortices have been removed. Only small monopole clusters survive. The density of monopoles ρ_{mon} is reduced by a factor 0.500 ± 0.003 . Combining this observation with the above-mentioned fact of strong correlation between monopoles in MAG and vortices in ICG we conclude that the removal of P-vortices gives rise to removal of almost all monopoles belonging to the infrared part of the monopoles. It is well known that the string tension vanishes in the modified ensemble.

In Fig. 2 the area spectrum of P-vortices, as it is found after ICG of the original ensemble, is compared with the spectrum that is obtained when the singular (monopole) part is subtracted from the Abelian projected gauge field after MAG, before the ICG is finally accomplished. Thereby the original vortex density $\rho_{\text{vort}} = 0.0805 \pm 0.0002$ is reduced to one fifth, $\rho_{\text{vort}} = 0.0162 \pm 0.0003$, without monopoles.

As long as the monopole fields are retained there is one big percolating vortex with an area of about 40,000 plaquettes present in each configuration (in addition to a lot of small size ones, with area $\lesssim 100$). After the monopole contributions to the Abelian field are removed the percolating P-vortex has disappeared from all configurations, the largest vortices being smaller in area than 6,000 plaquettes. Thus we observe that removing monopoles does not lead to the loss of all big P-vortices (which would be analogous to what happens to the monopoles after vortex removal), but rather to splitting of the single percolating P-vortex into a number of still relatively extended P-vortices.

The above results are in agreement with both scenarios of confinement, claiming

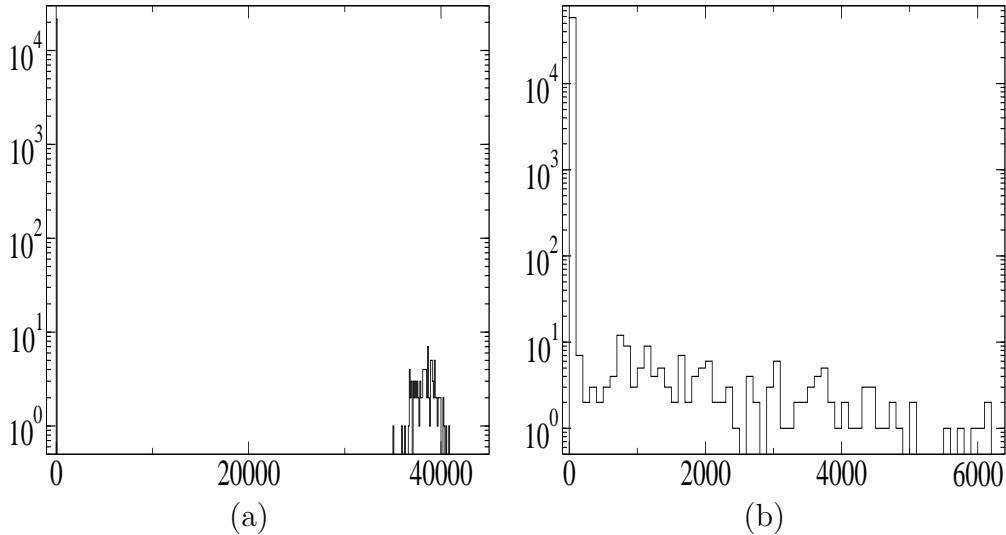


Figure 2: The area spectrum of center vortices for Wilson $\beta = 2.35$ on $24^3 \times 6$ lattices (a) for the original ensemble put into ICG, and (b) after monopoles have been removed.

that a non-vanishing string tension is due to percolating clusters of monopoles [40, 41] or due to the existence of percolating center vortices [44], respectively.

4 Direct center gauge: removing center vortices

When DCG fixing and center projection is completed, the vortex density is $\rho_{\text{vort}} = 0.0605 \pm 0.0002$. As we mentioned already in the Introduction we found something unexpected for the case of DCG, when center vortices are removed from the configurations. This is done in the following way. Each Monte Carlo configuration is gauge-fixed twice, to the MAG and to the maximal center gauge by DCG. The non-Abelian gauge field is then projected either to an Abelian $U(1)$ gauge field (from MAG) or to an $Z(2)$ gauge field (from DCG). In DCG, the remaining $Z(2)$ gauge freedom is exploited to reduce the number of negative ($Z_{x,\mu} = -1$) links.

In Ref.[14], de Forcrand and D’Elia noticed already the existence of a few percolating monopole clusters after the removal of vortices, clearly reduced in comparison to the amount of huge monopole clusters in the normal case. He mentioned, that only a handful of large clusters survives, whereas most of them are broken into pieces. Moreover, even the remaining largest clusters, according to his observation, did not contain monopole loops that wind around the periodic lattice. For the case of asymmetric lattices (finite temperature) considered in our work this observation would imply the absence of spatial winding. Qualitatively our results are in agreement with this expectation. Here we do not consider the winding number of the emerging monopole network clusters. Instead, we shall apply the decomposition of the clusters into non-intersecting monopole loops and find that none of them is spatially winding around the lattice.

Note that certain quantitative differences are possible due to the fact that DCG and MAG both are afflicted by their Gribov ambiguities. Our method differs from the method in Ref. [14] that we (*i*) always used the simulated annealing version of the gauge fixing procedure in question, *i.e.* we obtained higher local maxima

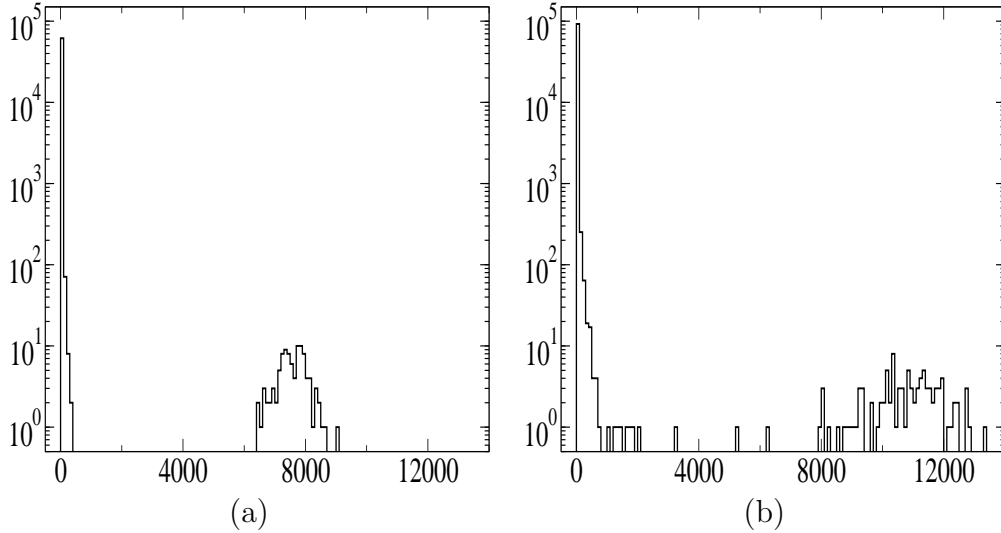


Figure 3: The same as Fig. 1, but (b) shows the situation after the center vortices found according to DCG have been removed.

for respective gauge fixing functionals, and (ii) the $Z(2)$ Landau gauge is realized. Both modifications are expected to lead to a minimal number of non-vanishing monopole currents and a minimal number of negative $Z(2)$ links, respectively. The realization of the $Z(2)$ Landau gauge has no effect on the monopole configuration. The procedure of P-vortex removal then requires the multiplication of each link by $Z_{x,\mu}$. This is applied not only to the original non-Abelian configuration but also to the Abelian projected configuration. In this way the monopole content of configurations with P-vortices removed can be easily compared with the monopole content of the original configuration. The monopole density ρ_{mon} is enhanced to $\rho_{\text{mon}} = 0.0551 \pm 0.0003$. We found, in particular, that the monopole clusters still contain a percolating component in agreement with Ref. [14].

The apparent paradox is demonstrated in Fig. 3 where the monopole cluster length spectrum before and after center vortex removal is compared. On the other hand, the non-Abelian string tension vanishes as it should [14] although only a minimal number of links has actually been changed. As expected in such a case, the monopole string tension also vanishes as it is shown in Fig. 4 where the non-Abelian and the monopole potentials before and after vortex removing are depicted.

Thus, monopole percolation is not sufficient to generate a confining potential. The monopole string tension, and consequently the Abelian string tension, may vanish if the percolating monopole cluster is highly correlated at small distances. In the following we will present several pieces of numerical evidence pointing out that the geometrical properties of monopole clusters after the removal of center vortices in DCG are indeed very different from the confining case.

(i) The number of selfintersections of the percolating cluster after removing of center vortices is substantially larger than before, as can be seen in Fig. 5 a.

(ii) A useful quantity to discriminate between confinement and deconfinement phases at finite temperature is suggested by the following fact. The monopole part $P^{\text{mon}}(\vec{x})$ of the Polyakov loop in any three-dimensional point \vec{x} is defined in eq. (3). Using eq. (13) one can express the monopole part $P^{\text{mon}}(\vec{x})$ as

$$P^{\text{mon}}(\vec{x}) = e^{i\Omega(\vec{x})/2}, \quad (6)$$

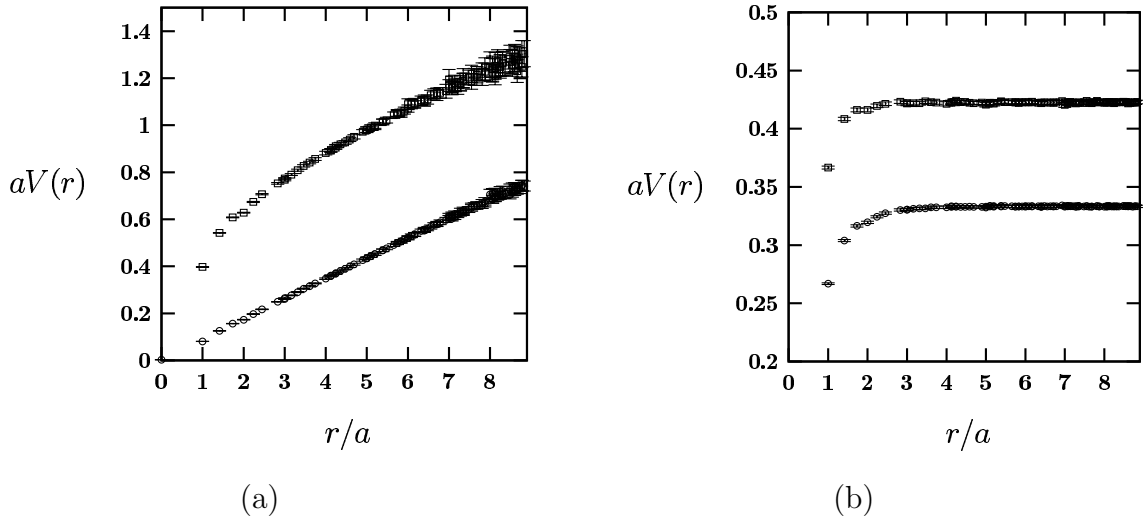


Figure 4: The non-Abelian potential ($aV(r)$, denoted by squares) and the monopole potential ($aV_{mon}(r)$, denoted by circles) at $\beta = 2.35$ on $24^3 \times 6$ lattices before (a) and after (b) removing of center vortices.

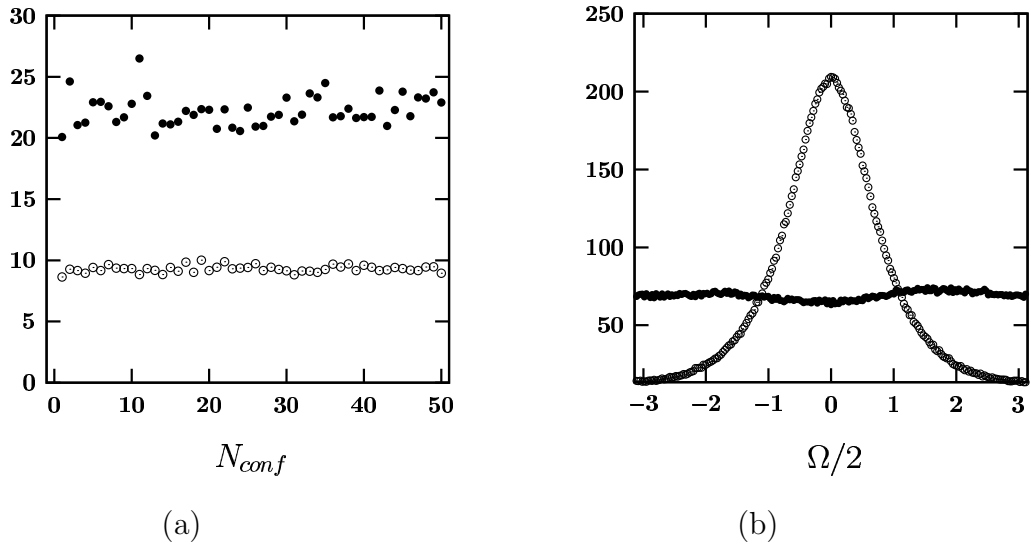


Figure 5: The ratio of the total length of the largest cluster to the number of crossings in it (a) and the solid angle Ω distribution (b) for normal configurations (full circles) and configurations free of center vortices (empty circles). The error bars in (b) are less than symbols.

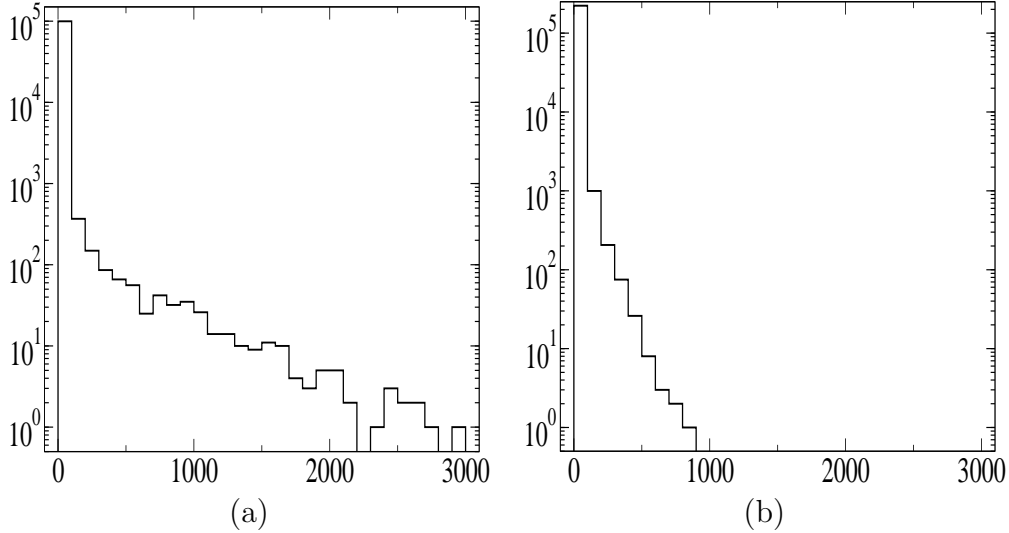


Figure 6: The length distribution $\tilde{N}(L)$ of irreducible loops emerging from the decomposition of monopole clusters, for $\beta = 2.35$ on 24^36 lattices in DCG before (a) and after (b) removing the center vortices.

where $\Omega(\vec{x})$ is the solid angle of all monopole trajectories (projected onto a single time slice, with proper regard of the direction of the monopole current) as monitored from the locus \vec{x} of the Polyakov loop (thought to be located in the same time slice).

$\Omega(\vec{x})$ has been introduced as an observable characterizing the difference between the confinement and deconfinement phase in Ref. [47]. It has turned out that the distribution of the local values $\Omega(\vec{x})$ (the histogram summed over all configurations of an ensemble) is flat in confinement and has a Gaussian form in the case of deconfinement. Fig. 5 b shows the distributions of $\Omega(\vec{x})$ as found for normal confining configurations and for the ensemble cleaned from center vortices. The distribution for the latter is qualitatively very similar to that in the deconfinement phase.

(iii) In order to describe the correlations within the apparently percolating monopole clusters, it is useful to decompose the cluster by subtracting from bigger clusters closed, oriented and irreducible (non-selfintersecting) loops, stepping up in loop size (lengths of 4, 6, 8 etc.) until nothing remains to be subtracted. The result of this procedure can be presented as a histogram $\tilde{N}(L)$ of irreducible loops (with respect to the loop size) in place of the histogram $N(L)$ of connected clusters (with respect to the length of monopole currents inside the clusters). Fig. 6 is the analog to Fig. 3, showing now the respective *loop length distributions*. It turns out from comparing Figs. 6 and 3 that the percolating but non-confining monopole clusters can be completely decomposed into loops of comparably small size. The irreducible monopole loops of the original ensemble (before removing center vortices) ranges to three times larger loops. Among them are such wrapping around the lattice.

This result is corroborated by the following random simulation of non-confining, yet percolating monopole clusters. We have tried to model the monopole configurations left over after removal of vortices by a random gas of small monopole loops. Such configurations were created by the following procedure. A set of N_{DPL} Dirac plaquettes were put on the lattice with randomly chosen location in a randomly chosen plane, with random sign of $m_{x,\mu\nu}$. In Fig. 7 the resulting distribution of $\Omega(\vec{x})$ and the static potential are shown for $N_{DPL} = 6,000$. For this number of Dirac plaquettes we find as the result of the procedure that a large connected monopole

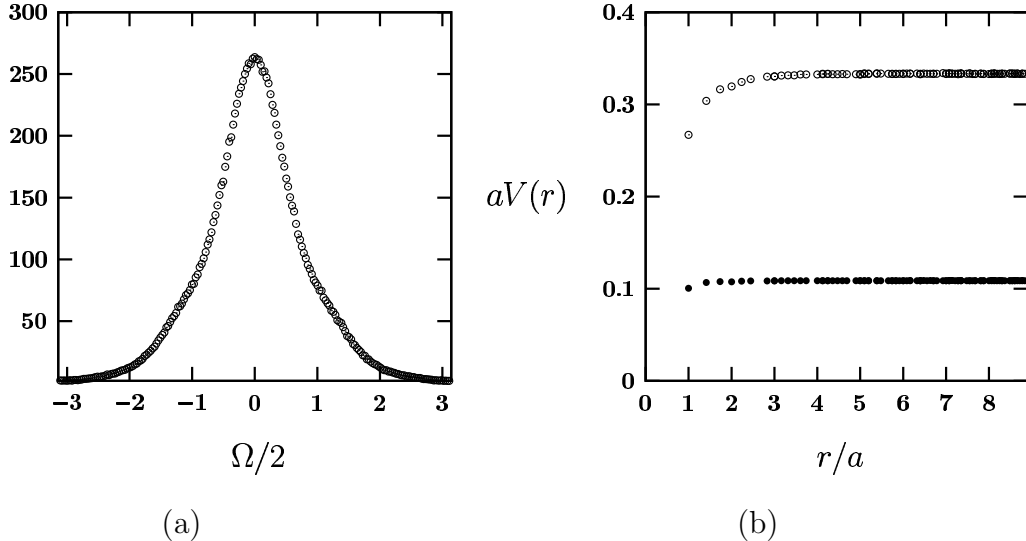


Figure 7: The solid angle Ω distribution (a) for a random monopole configurations obtained as described in the text and the static monopole-generated potential (b) for these configurations (full circles) compared with the ensemble free of center vortices (empty circles). Error bars are within symbol size.

cluster of a length of $O(10,000)$ has grown up and the total number of monopole currents (including also smaller clusters) is close to that in the P-vortex-removed configurations. In Fig. 7 one can see that both the distribution of $\Omega(\vec{x})$ and the static potential are qualitatively similar to those in the ensemble of configurations free of center vortices.

The facts (i), (ii) and (iii) show that percolating monopole clusters, unexpectedly appearing in configurations without P-vortices and without confinement, are really highly correlated at small distances and that this can be directly related to the lack of confinement. The simulation based on independent 1×1 Dirac plaquettes shows that this might be an almost realistic model of how these clusters could have been randomly created.

5 Direct center gauge: removing monopoles

Finally, we describe what effect the removal of Abelian monopoles has on the P-vortex content in DCG. The basic ensemble of configurations has been put into the MAG with the help of the simulated annealing method. From the Abelian projected gauge field the singular (monopole) part has been removed before the *modified* non-Abelian field has been reconstructed using the coset part left out in the Abelian projection. This is explained in Eqs. (13), (14) and (15) in the Appendix. Finally we put the two lattice fields into DCG and view the corresponding P-vortex content. The P-vortex density $\rho_{\text{vort}} = 0.0605 \pm 0.0002$ (*i. e.* the total vortex area relative to the total number of plaquettes in the lattice) of the ensemble with monopoles is reduced to $\rho_{\text{vort}} = 0.0131 \pm 0.0002$ (*i. e.* roughly one fifth of the original density) in the ensemble where monopoles have been removed. In Fig. 8 we compare the area distribution of *individual* center vortices after monopole removal (b) with the original distribution obtained without modifying the gauge fields (a). This Figure is very much similar to Fig. 2 obtained in ICG. While Fig. 8a shows a significant part

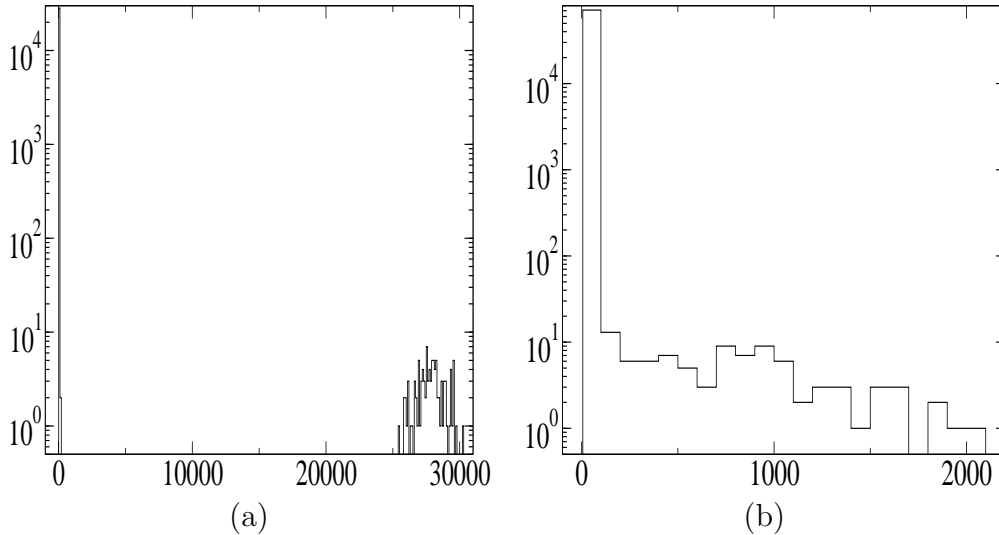


Figure 8: The same as Fig. 2 but with vortices defined in DCG, (a) before and (b) after monopoles have been removed.

of clusters with very large area consisting of more than $O(20,000)$ dual plaquettes, after monopole removal such large clusters do not occur any more. The largest ones have an area less by one order of magnitude in the number of dual plaquettes and cannot be isolated from the smallest vortices occurring in the area distribution. This corresponds to our expectation.

Fig. 9 shows the contribution of center vortices to the quark-antiquark potential in DCG before (upper linearly rising curve) and after removal of Abelian monopoles (lower flat curve). This picture clearly shows that the left-over, comparably short-ranged center vortices do not provide a confining potential.

6 Conclusions

In this paper we have tried to give an answer to the question of the mutual interdependence of the two types of topological gauge field fluctuations, condensation of which is popularly held responsible for quark confinement: center vortices (more precisely, P-vortices) and Abelian monopoles. For this we have applied techniques of respective removal of one type of these fluctuations in order to study the result with respect to the other type. Center vortices were identified within the projected $Z(2)$ gauge field obtained in two ways: (i) from the indirect center gauge, where the maximally Abelian gauge is applied as a first step and the (Abelian) maximal center gauge is fixed within the residual Abelian gauge symmetry, before the projection to the center subgroup $Z(2)$ is made, and (ii) through the direct maximally center gauge achieved within the non-Abelian gauge freedom. Abelian monopoles were throughout studied within the maximally Abelian gauge. The gauges were iteratively fixed with the help of a simulated annealing algorithm, which - when applied to the consecutive step of complimentary gauge fixing - has erased the memory with respect to the first step of gauge fixing.

We have found a clear correlation between both types of objects. We confirm that the removal of each of these types leads to a loss of confinement described in terms of the other type, respectively. However, in case of removing P-vortices detected

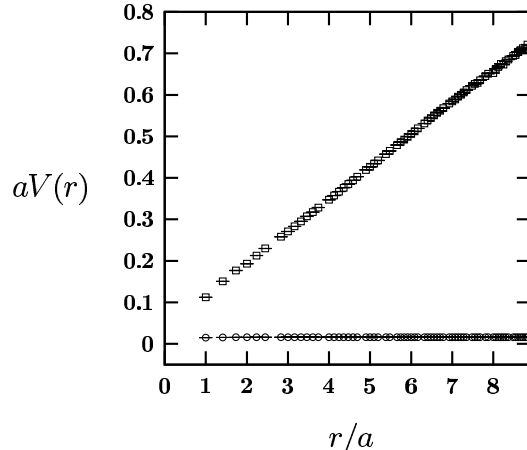


Figure 9: The center vortex contribution to the quark-antiquark potential, rising for the original ensemble put into DCG (denoted by squares), flat for DCG after Abelian monopoles have been removed (denoted by circles).

within the direct center gauge, we found much more monopole currents and larger (spanning) monopole clusters than seen before P-vortex removal. A closer inspection showed that these monopole clusters are strongly correlated at short range such that they are reducible into a large number of considerably short monopole loops, the latter not contributing to a linearly rising confinement potential. This somewhat surprising observation shows, that spatial percolation of infrared monopole clusters alone is not a sufficient condition for *real* monopole condensation and thus for quark confinement (for the connection of the latter see Ref. [48, 33]).

We have restricted our investigations to the case of just one temperature value within the confinement phase. We are convinced that this does not represent a real loss of generality as long as $T < T_c$.

Appendix

Here we give the standard definitions for $SU(2)$ lattice gauge theory which we have used in the studies described in the text. We perform our analyses both in the Direct [4] – and in the Indirect [2] – Maximal Center Gauges (DCG and ICG). The DCG in $SU(2)$ lattice gauge theory is defined by the maximization of the functional

$$F_1(U) = \sum_{x,\mu} (\text{Tr } g U_{x,\mu})^2, \quad (7)$$

with respect to gauge transformations $g \in SU(2)$. $U_{x,\mu}$ is the lattice gauge field and $g U_{x,\mu} = g^\dagger(x) U_{x,\mu} g(x + \hat{\mu})$ the gauge transformed lattice gauge field. Maximization of (7) fixes the gauge up to $Z(2)$ gauge transformations, and the corresponding, projected $Z(2)$ gauge field is defined as:

$$Z_{x,\mu} = \text{sign}(\text{Tr } g U_{x,\mu}). \quad (8)$$

After this identification is made, one can make use of the remaining $Z(2)$ gauge freedom in order to maximize the $Z(2)$ gauge functional

$$F_2(Z) = \sum_{x,\mu} z Z_{x,\mu} \quad (9)$$

with respect gauge transformations $z(x) \in Z(2)$, $Z_{x,\mu} \rightarrow {}^z Z_{x,\mu} = z^*(x)Z_{x,\mu}z(x + \hat{\mu})$. This is the $Z(2)$ equivalent of the Landau gauge. In distinction to Ref. [14], this final step is automatically understood here before the vortex removal operation (to be defined below) is done.

The ICG goes an indirect way. At first, one fixes the maximally Abelian gauge (MAG) by maximizing the functional

$$F_3(U) = \sum_{x,\mu} \text{Tr} \left({}^g U_{x,\mu} \sigma_3 ({}^g U_{x,\mu})^\dagger \sigma_3 \right), \quad (10)$$

with respect to gauge transformations $g \in SU(2)$. The maximization fixes the gauge up to $g \in U(1)$. Therefore, the following projection to an $U(1)$ gauge field through the phase of the diagonal elements of the links, $\theta_{x,\mu} = \arg \left(({}^g U_{x,\mu})^{11} \right)$, is not unique. The non-Abelian link field is split according to $U_{x,\mu} = u_{x,\mu} V_{x,\mu}$ in an Abelian (diagonal) part $u_{x,\mu} = \text{diag} \{ \exp(i\theta_{x,\mu}), \exp(-i\theta_{x,\mu}) \}$ and a coset part $V_{x,\mu} \in SU(2)/U(1)$, the latter representing non-diagonal gluons. Exploiting the remaining $U(1)$ gauge freedom, which amounts to a shift $\theta_{x,\mu} \rightarrow {}^\alpha \theta_{x,\mu} = -\alpha(x) + \theta_{x,\mu} + \alpha(x + \hat{\mu})$, one can maximize the Abelian gauge functional

$$F_4(u) = \sum_{x,\mu} (\cos({}^\alpha \theta_{x,\mu}))^2, \quad (11)$$

that serves the same purpose as (7). Finally, the projected $Z(2)$ gauge field is defined as

$$Z_{x,\mu} = \text{sign}(\cos({}^\alpha \theta_{x,\mu})). \quad (12)$$

This second step in ICG is completely analogous to the DCG case, in other words one maximizes $F_1(U)$ in Eq. (7), however for all $U_{x,\mu}$ restricted to the projected links $u_{x,\mu} = \text{diag} \{ \exp(i\theta_{x,\mu}), \exp(-i\theta_{x,\mu}) \}$, admitting only $U(1)$ gauge transformations denoted by α . The $Z(2)$ gauge variables are used to form $Z(2)$ plaquettes. Most of them are equal to +1, typically 30,000 plaquettes are equal to -1 after center projection via DCG (and 40,000 after center projection via ICG, respectively). The P-vortex surfaces are actually formed by plaquettes *dual* to the negative plaquettes. The vortex density is therefore $\rho_{\text{vort}} = 0.0605 \pm 0.0002$ and $\rho_{\text{vort}} = 0.0805 \pm 0.0002$ in DCG and ICG, respectively.

In order to fix the maximally Abelian and the direct maximal center gauge we have created 10 randomly gauge transformed copies of the original gauge field configuration and applied the Simulated Annealing algorithm [10] to find the optimal non-Abelian gauge transformation g . We have used for further analyses always *that* copy ${}^g U$ (or ${}^\alpha \theta$) which corresponds to the maximal value of the respective gauge fixing functional. In order to perform the second step of the indirect maximal center gauge via configurations, that have been first fixed to the maximally Abelian gauge and projected to $U(1)$ fields u , we have started again from 10 random *Abelian gauge transforms* of the latter.

We have used the standard DeGrand–Toussaint definition [49] of monopole currents defined by the phase $\theta_{x,\mu}$ of $u_{x,\mu}$. The typical number of monopole currents per configurations amounts to 12,000 dual links, corresponding to a density of $\rho_{\text{mon}} = 0.0357 \pm 0.0002$. The part of the Abelian gauge field originating from the monopoles is

$$\theta_{x,\mu}^{\text{mon}} = -2\pi \sum_{x'} D(x - x') \partial'_\nu m_{x',\nu\mu}. \quad (13)$$

Here $D(x)$ is the inverse lattice Laplacian, and ∂'_μ is the lattice backward derivative. The Dirac sheet variable, $m_{x,\mu\nu}$, is defined as the integer multiple of 2π part of the

plaquette angle $\theta_{x,\mu\nu}$, whereas the reduced plaquette angle $\bar{\theta}_{x,\mu\nu} \in (-\pi, \pi]$ is the fractional part: $\theta_{x,\mu\nu} = 2\pi m_{x,\mu\nu} + \bar{\theta}_{x,\mu\nu}$. The Abelian gauge field with monopoles removed is defined as [13]:

$$u_{x,\mu}^{monopole\ removed} = (u_{x,\mu}^{mon})^\dagger u_{x,\mu}, \quad (14)$$

where $u_{x,\mu}^{mon} = \text{diag} \{ \exp(i\theta_{x,\mu}^{mon}), \exp(-i\theta_{x,\mu}^{mon}) \}$. Upon multiplication with the coset field $V_{x,\mu}$, this holds also for the non-Abelian links

$$U_{x,\mu}^{monopole\ removed} = (u_{x,\mu}^{mon})^\dagger U_{x,\mu}. \quad (15)$$

Analogously the gauge fields with the P-vortices removed are defined as [14]:

$$U_{x,\mu}^{vortex\ removed} = Z_{x,\mu} U_{x,\mu}, \quad (16)$$

where $Z_{x,\mu}$ is given by (8).

Acknowledgements

The authors want to thank M.N. Chernodub for valuable discussions and Ph. de Forcrand for useful remarks on a first version of this paper. The work was partially supported by grants RFBR-DFG 06-02-04010 and DFG-RFBR 436 RUS 113/739/2. The ITEP group (A.I.V., B.V.M., M.I.P., V.G.B., A.V.K. and P.Yu.B.) was partially supported by grants RFBR 06-02-16309, 05-02-16306, 05-02-17642 and 04-02-16079, and by the EU Integrated Infrastructure Initiative Hadron Physics (I3HP) under contract RII3-CT-2004-506078. The work of E.-M.I. is supported by DFG through the Forschergruppe FOR 465 (Mu932/2).

References

- [1] H. Shiba and T. Suzuki, Phys. Lett, **B 333** (1994) 461.
- [2] L. Del Debbio, M. Faber, J. Greensite, and S. Olejnik, Phys. Rev. **D55** (1997) 2298.
- [3] M. Faber, J. Greensite, and S. Olejnik, Phys. Rev. **D57** (1998) 2603.
- [4] L. Del Debbio, M. Faber, J. Giedt, J. Greensite, and S. Olejnik, Phys. Rev. **D58** (1998) 094501.
- [5] K. Langfeld, H. Reinhardt, and O. Tennert, Phys. Lett. **B 419** (1998) 317.
- [6] K. Langfeld, O. Tennert, M. Engelhardt, and H. Reinhardt, Phys. Lett. **B 452** (1999) 301.
- [7] M. Engelhardt, K. Langfeld, H. Reinhardt, and O. Tennert, Phys. Rev. **D61** (2000) 054504.
- [8] J. M. Cornwall, Phys. Rev. **D73** (2006) 065004.
- [9] J. Greensite, Prog. Part. Nucl. Phys. **51** (2003) 1.
- [10] G. S. Bali, V. Bornyakov, M. Müller-Preussker, and K. Schilling, Phys. Rev. **D54** (1996) 2863.
- [11] V. G. Bornyakov, D. A. Komarov and M. I. Polikarpov, Phys. Lett. **B497** (2001) 151.

- [12] O. Miyamura, Phys. Lett. **B353** (1995) 91.
- [13] S. Sasaki and O. Miyamura, Nucl. Phys. Proc. Suppl. **63** (1998) 507, Phys. Lett. **B443** (1998) 331, Phys. Rev. **D59** (1999) 094507.
- [14] P. de Forcrand and M. D'Elia, Phys. Rev. Lett. **82** (1999) 4582.
- [15] J. M. Cornwall, Phys. Rev. **D61** (2000) 085012, Phys. Rev. **D65** (2002) 085045.
- [16] J. Ambjorn, J. Giedt, and J. Greensite, JHEP **0002** (2000) 033.
- [17] A. V. Kovalenko, M. I. Polikarpov, S. N. Syritsyn, and V. I. Zakharov, Nucl. Phys. Proc. Suppl. **129** (2004) 665.
- [18] A. V. Kovalenko, M. I. Polikarpov, S. N. Syritsyn, and V. I. Zakharov, Phys. Rev. **D71** (2005) 054511.
- [19] A. V. Kovalenko, M. I. Polikarpov, S. N. Syritsyn, and V. I. Zakharov, Phys. Lett. **B613** (2005) 52.
- [20] P. de Forcrand and M. Pepe, Nucl. Phys. **B598** (2001) 557.
- [21] K. Langfeld, H. Reinhardt, and A. Schäfer, Phys. Lett. **B504** (2001) 338.
- [22] B. Lucini and M. Teper, JHEP **0106** (2001) 050.
- [23] B. Lucini, M. Teper, and U. Wenger, JHEP **0401** (2004) 061.
- [24] G. 't Hooft, in *High Energy Physics*, edited by A. Zichichi, Editrice Compositore, Bologna. 1976.
- [25] S. Mandelstam, Phys. Reports **23C** (1976) 245.
- [26] G. 't Hooft, Nucl. Phys. **B190** [FS3] (1981) 455.
- [27] A. S. Kronfeld, M. L. Laursen, G. Schierholz, and U. J. Wiese, Phys. Lett. **B198** (1987) 516.
- [28] T. Suzuki and I. Yotsuyanagi, Phys. Rev. **D42** (1990) 4257.
- [29] J. Fröhlich and P. A. Marchetti, Commun. Math. Phys. **112** (1987) 343.
- [30] L. Del Debbio, A. Di Giacomo, and G. Paffuti, Phys. Lett. **B349** (1995) 513; L. Del Debbio, A. Di Giacomo, G. Paffuti, and P. Pieri, Phys. Lett. **B355** (1995) 255.
- [31] A. I. Veselov, M. I. Polikarpov, and M. N. Chernodub, JETP Lett. **63** (1996) 411; M. N. Chernodub, M. I. Polikarpov, and A. I. Veselov, Phys. Lett. **B399** (1997) 267.
- [32] J. Fröhlich and P. A. Marchetti, Phys. Rev. **D64** (2001) 014505.
- [33] V.A. Belavin, M.N. Chernodub, and M.I. Polikarpov, JETP Lett. **75** (2002) 217, Phys. Lett. **B554** (2003) 146.
- [34] V. G. Bornyakov, E.-M. Ilgenfritz, M. L. Laursen, V. K. Mitrjushkin, M. Müller-Preussker, A. J. van der Sijs, and A. M. Zadorozhnyi, Phys. Lett. **B261** (1991) 116.
- [35] V. G. Bornyakov and M. Müller-Preussker, Nucl. Phys. Proc. Suppl. **106** (2002) 646.
- [36] V. G. Bornyakov, E.-M. Ilgenfritz, and M. Müller-Preussker, Phys. Rev. **D72** (2005) 054511.
- [37] T. L. Ivanenko, A. V. Pochinsky, and M. I. Polikarpov, JETP Lett. **53** (1991) 543, Phys. Lett. **B302** (1993) 458.

- [38] V. G. Bornyakov, V. K. Mitrjushkin, and M. Müller-Preussker, Phys. Lett. **B284** (1992) 99.
- [39] S. i. Kitahara, Y. Matsubara and T. Suzuki, Prog. Theor. Phys. **93** (1995) 1.
- [40] A. Hart and M. Teper, Phys. Rev. **D58** (1998) 014504.
- [41] A. Hart and M. Teper [UKQCD Collaboration], Phys. Rev. **D60** (1999) 114506.
- [42] J. D. Stack, S. D. Neiman, and R. J. Wensley, Phys. Rev. **D50** (1994) 3399.
- [43] J. D. Stack, R. J. Wensley, and S. D. Neiman, Phys. Lett. **B385** (1996) 261.
- [44] R. Bertle, M. Faber, J. Greensite, and S. Olejnik, JHEP **9903** (1999) 019.
- [45] M. N. Chernodub, M. I. Polikarpov, A. I. Veselov, and M. A. Zubkov, Nucl. Phys. Proc. Suppl. **73** (1999) 575.
- [46] M. Engelhardt and H. Reinhardt, Nucl. Phys. **B585** (2000) 591.
- [47] S. Ejiri, S. i. Kitahara, Y. Matsubara, T. Okude, T. Suzuki, and K. Yasuta, Nucl. Phys. Proc. Suppl. **47** (1996) 322.
- [48] A. Di Giacomo, Acta Phys. Polon. **B36** (2005) 3723 and references therein.
- [49] T. A. DeGrand and D. Toussaint, Phys. Rev. **D22** (1980) 2478.